

EMF Compliance Assessments of 5G Devices

Serge Pfeifer, IT'IS Foundation

Esra Neufeld, IT'IS Foundation

Eduardo Carrasco, IT'IS Foundation

Andreas Christ, IT'IS Foundation

Myles Capstick, IT'IS Foundation

Sven Kühn, IT'IS Foundation

Katja Pokovic, SPEAG

Theodore Samaras, AUTH

Q. Balzano, University of Maryland

Niels Kuster, IT'IS Foundation & ETH Zurich

5G Workshop, BioEM 2018, June 24, 2018



ETH

Eidgenössische Technische Hochschule Zürich
Swiss Federal Institute of Technology Zurich

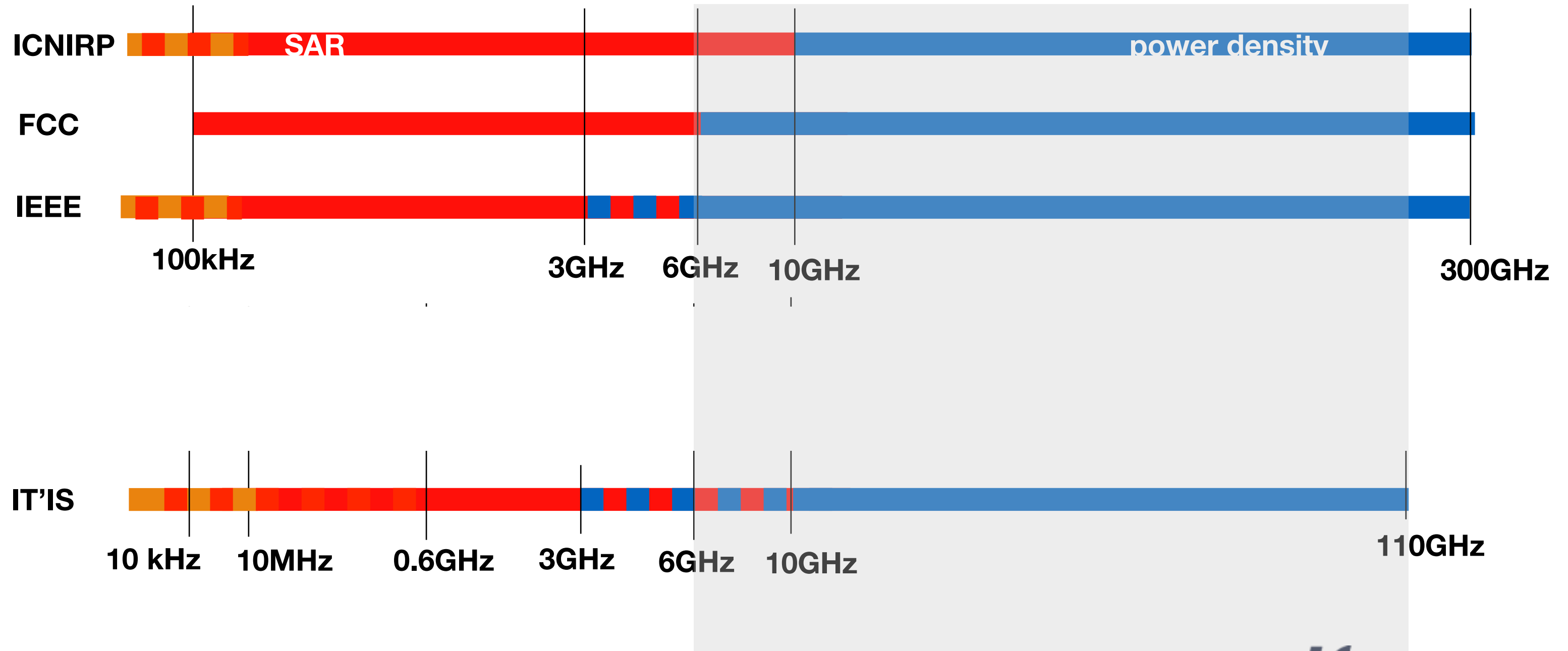
IT'IS FOUNDATION

Content

- Solutions Based on Forward and Backward Propagation
- Solutions Based on Direct Measurement
- Calibration 10 – 110 GHz
- Scanning and Field Reconstruction
- Worst-Case Phase Assessment
- Verification Sources
- Uncertainty Budget
- System Validation
- Combination of SAR & Power Density
- Conclusions

EM Safety Guidelines / Regulation and Open Issues

EM Safety Guidelines / Regulation



Theoretical and Numerical Assessment of Maximally Allowable Power-Density Averaging Area for Conservative 5G Exposure Assessment

Esra Neufeld¹, Eduardo Carrasco¹, Quirino Balzano^{1,3}, Andreas Christ¹, Niels Kuster^{1,2}

¹ Foundation for Research on Information Technologies in Society (IT'IS), Zeughausstr. 43, 8004 Zurich, Switzerland

² Swiss Federal Institute of Technology (ETH) Zurich, 8092 Zurich, Switzerland

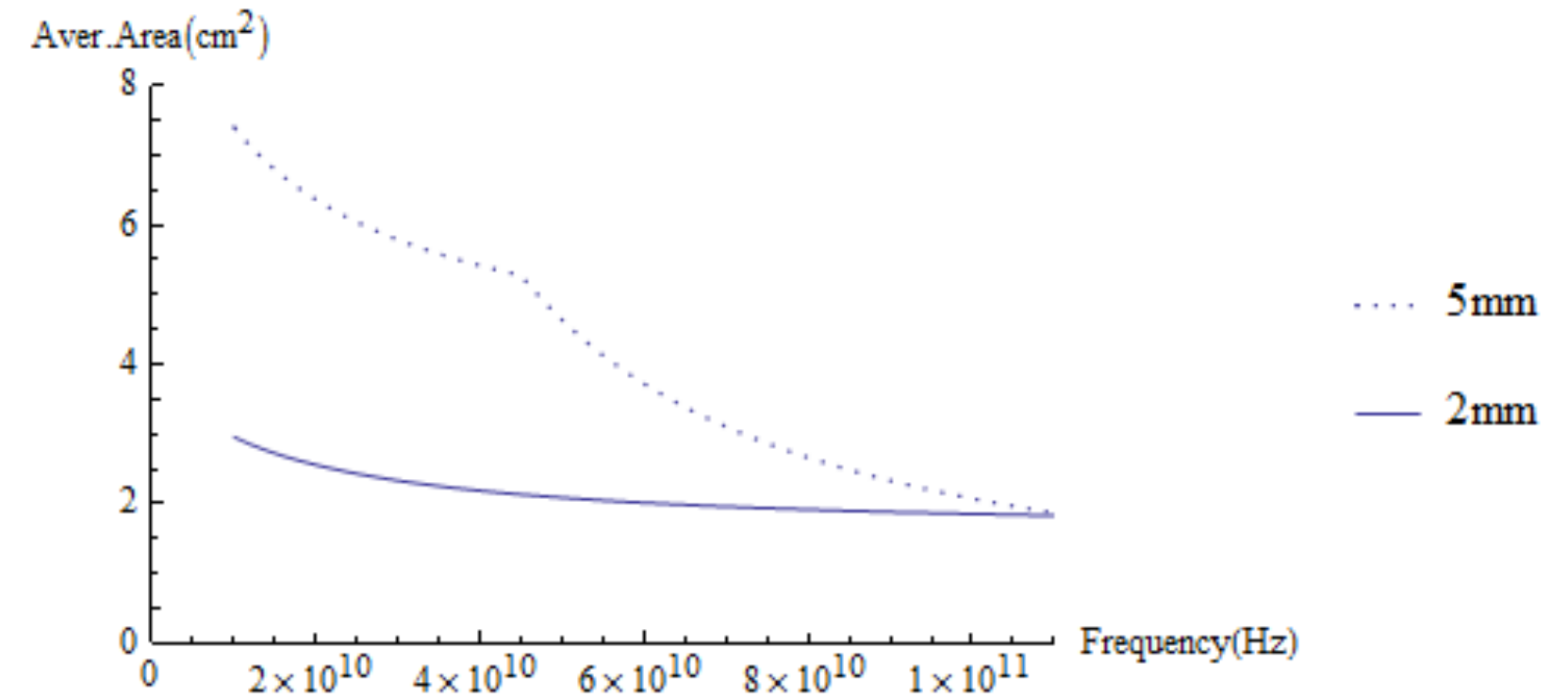
³ Department of Electrical and Computer Engineering, University of Maryland, College Park, MD, USA

Abstract. The objective of this paper is to determine a maximum averaging area for power density that limits the maximum temperature increase to 1 K for frequencies above 6 GHz. This maximum area should be conservative for any transmitter at any distance of >2 mm from the field generating sources (primary transmitting antennas or secondary field sources). To derive a generically valid maximum averaging area, an analytical approximation for the peak temperature increase by localized exposure has been derived (based on Green's functions, transfer coefficient computation, and a relationship between wavelength (λ), source-distance (d), and beam-width as a function of antenna aperture / reflector radius), under the assumptions that exposure can be conservatively approximated as Gaussian and that penetration depth is negligible.

Results

■ the theoretical model determines a maximal averaging area for 1K, 10 W/m² that depends on distance, frequency, and antenna aperture (in the far-field only, set to 5cm in graphs)

■ **THU, S13-2 [15:45]**



Systematic Derivation of Safety Limits for Time Varying 5G Radiation Exposure Based on Analytical Models and Thermal Dose

Esra Neufeld¹, Nils Kuster^{1,2}

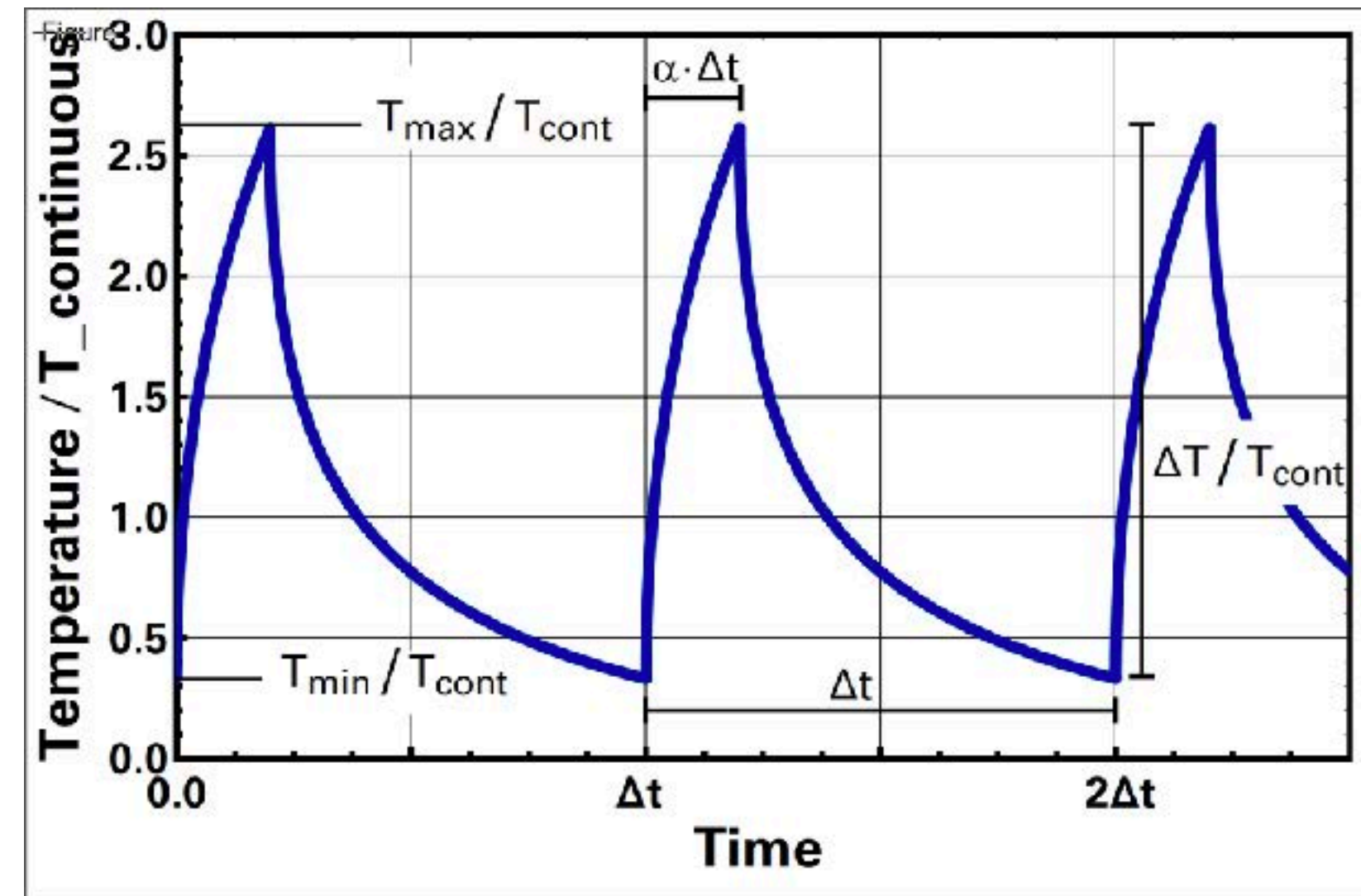
¹ Foundation for Research on Information Technologies in Society (IT'IS),
Zeughausstr. 43, 8004 Zurich, Switzerland

² Swiss Federal Institute of Technology (ETH) Zurich, 8092 Zurich, Switzerland

Abstract. Very broadband wireless devices operating above 10 GHz may transmit data in bursts of a few millisecond to seconds. Even though the time- and area-averaged power density values remain within the acceptable safety limits for continuous exposure, these bursts may lead to short temperature spikes in the skin of exposed people. In this paper a novel analytical approach to pulsed heating is developed and applied to assess the temperature peak to average temperature ratio as a function of the pulse fraction α (relative to the averaging time ΔT ; it corresponds to the inverse of the peak-to-average ratio (PAR)). This has been analyzed for two different perfusion-related time constants ($\tau_1 = 100$ s and 500 s) corresponding to plane wave and localized exposures. In order to allow peak temperatures considerably exceeding the 1 K increase, the CEM43 tissue damage model with an experimental data-based damage threshold for human skin of 600 min is used to allow large temperature

Results

- temperature oscillations become very large ($\gg 10$) for PAR in the order of 1000
- based on thermal damage measures, this would result in unacceptable exposure duration limitations
- accepting a 4K temperature increase for continuous prevents any modulation
- for a 1K continuous exposure increase one obtains for the averaging time:
 - e.g., 5s for $\text{PAR} < 1000$, 30s for $\text{PAR} < 100$, 4min for $\text{PAR} < 4$
- the research indicates that exposures with modulations tissue damage cannot be excluded applying the limits of 1998
- publication accepted by health physics
- **FRI S16-6 [10:45]**

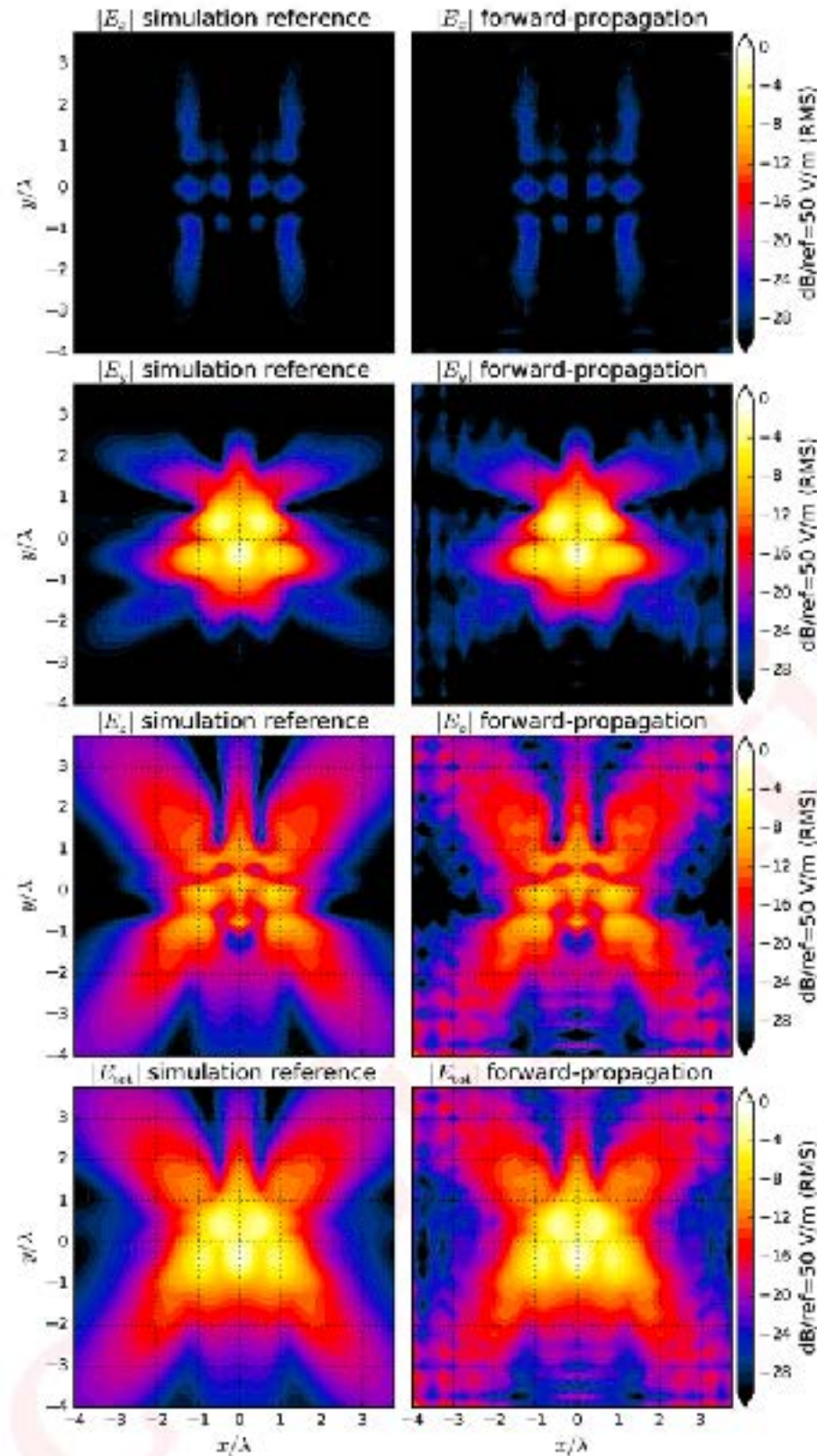


$\Delta t = \tau_1$ (100s - 500s) and $\alpha = 20\%$ (average 1 K)

Solutions Based on Forward and Backward Propagation

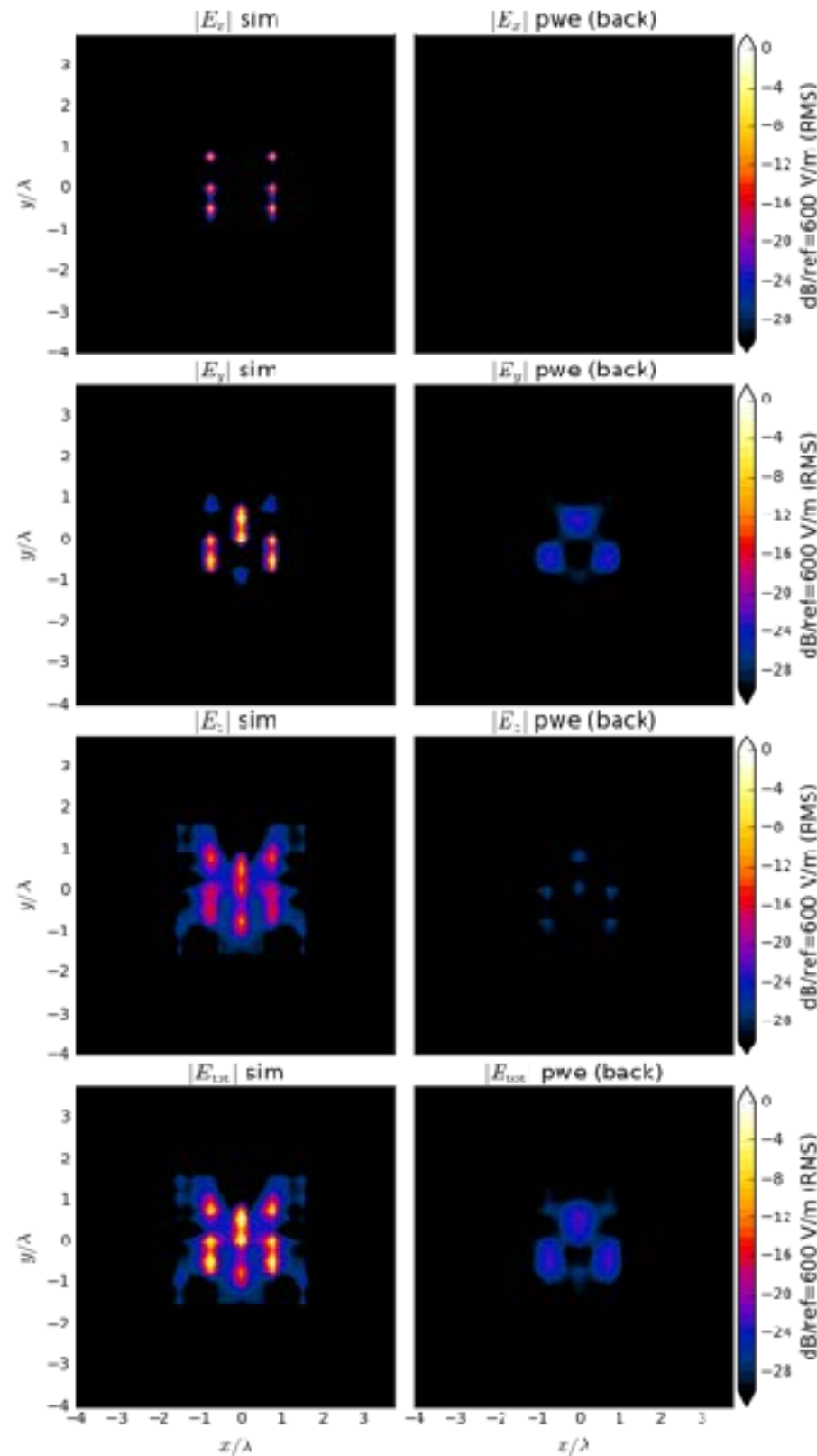
Forward Propagation (Away from the Source)

- straight forward
- works very accurately
 - example from 2 – 5 mm
- small uncertainty
- saves measurement time



Backward Propagation (Towards the Source)

- information about reactive fields and evanescence fields are missing
- backward propagation falls apart very close to the source
 - example from 2 mm to 0.1 mm
- unreliable with uncertainties > 10 dB
- cannot be used for compliance testing



Conclusion

- forward propagation: low uncertainty
- backward propagation: very high uncertainty when backward propagated into the reactive near-field

Solutions Based on Direct Measurement

Measurement by E-Field and H-Field Probes

■ E-field probes

■ challenges

- ▶ field distortions by substrates / probe body
- ▶ directionality

■ H-field probes

■ challenges

- field distortion/scattering by probe body
- E-field sensitivity

■ elctro-/magneto-optical probes

■ challenges

- spatial resolution
- sensitivity

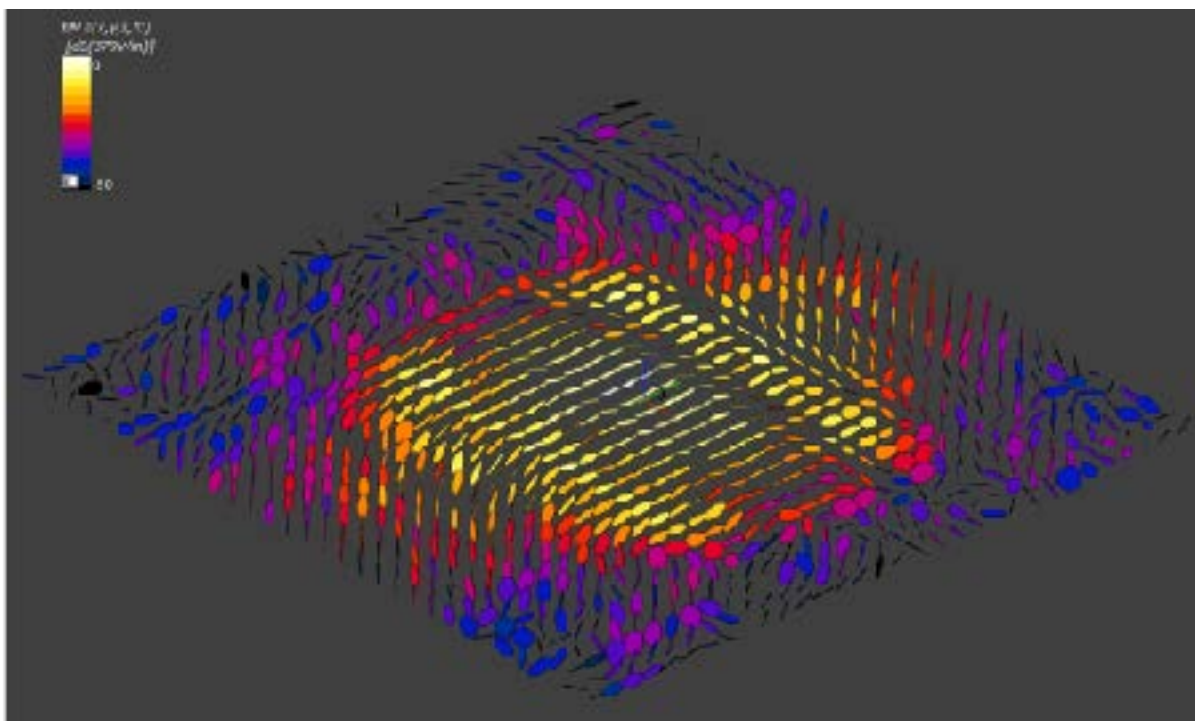
■ wave-guide

■ challenges

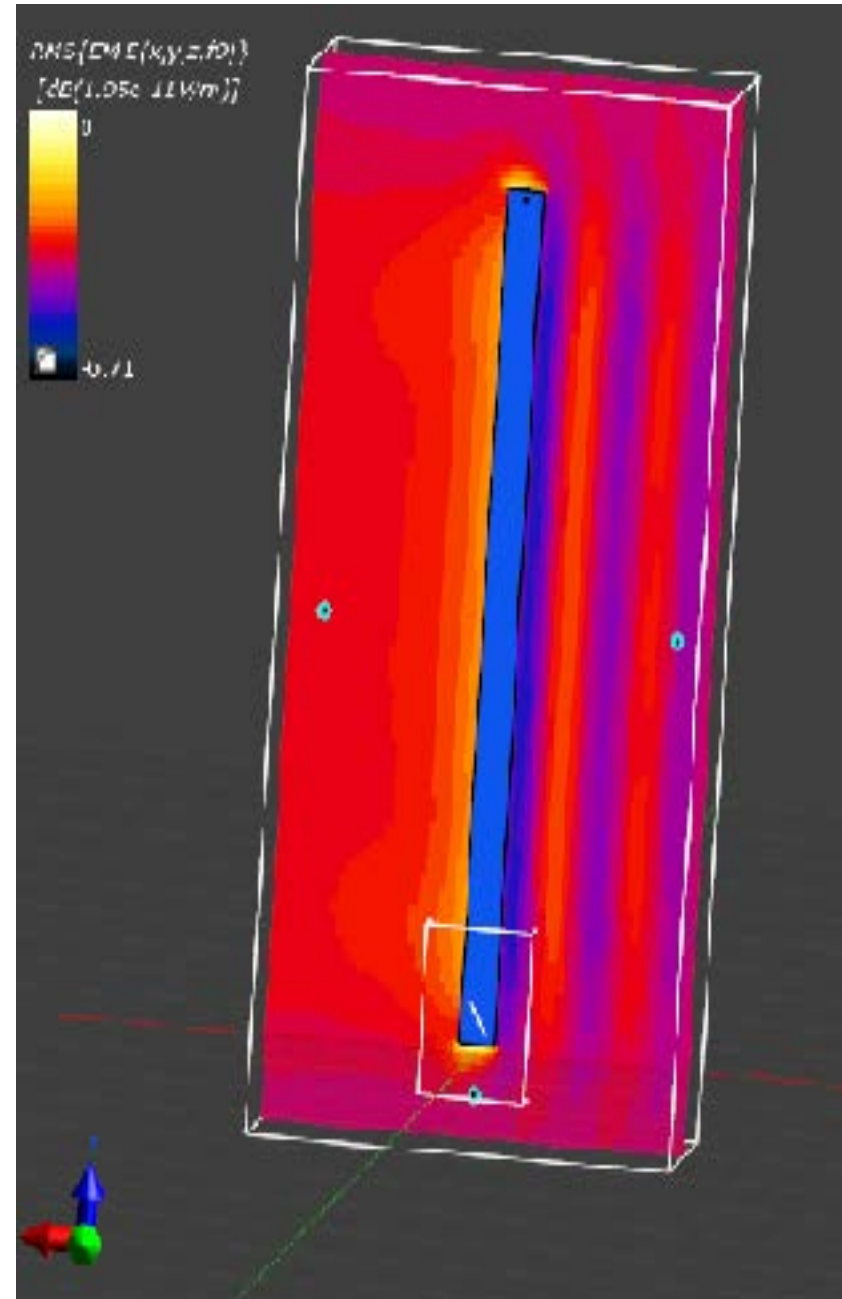
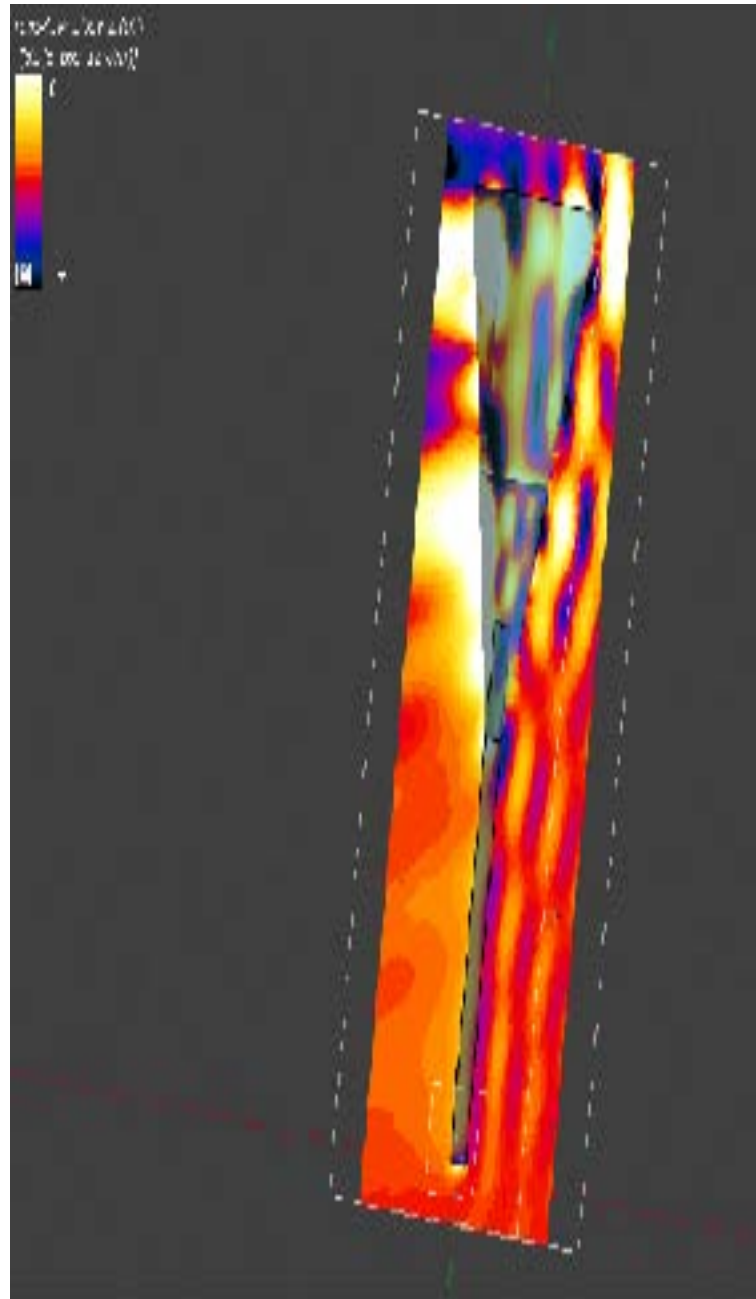
- large field distortions
- fixed impedance

EUmmWV2 Probe: Pseudo-Vector Design

- probe
 - 2 dipoles (one each side of the quartz substrate)
 - ≈ 0.9 mm long and diode loaded
 - typical distance between physical tip and sensor center: 1.5 mm
- quartz substrate
 - 0.9 mm wide
 - 20 mm long
 - 0.18 mm thick
 - dipole sensors present
 - $\epsilon_r = 3.8$ (quartz) homogeneous
- measurement: three rotations around axis, (i.e., 6 E-field measurements in total)
- reconstruction of ellipse and elimination of mechanical tolerances

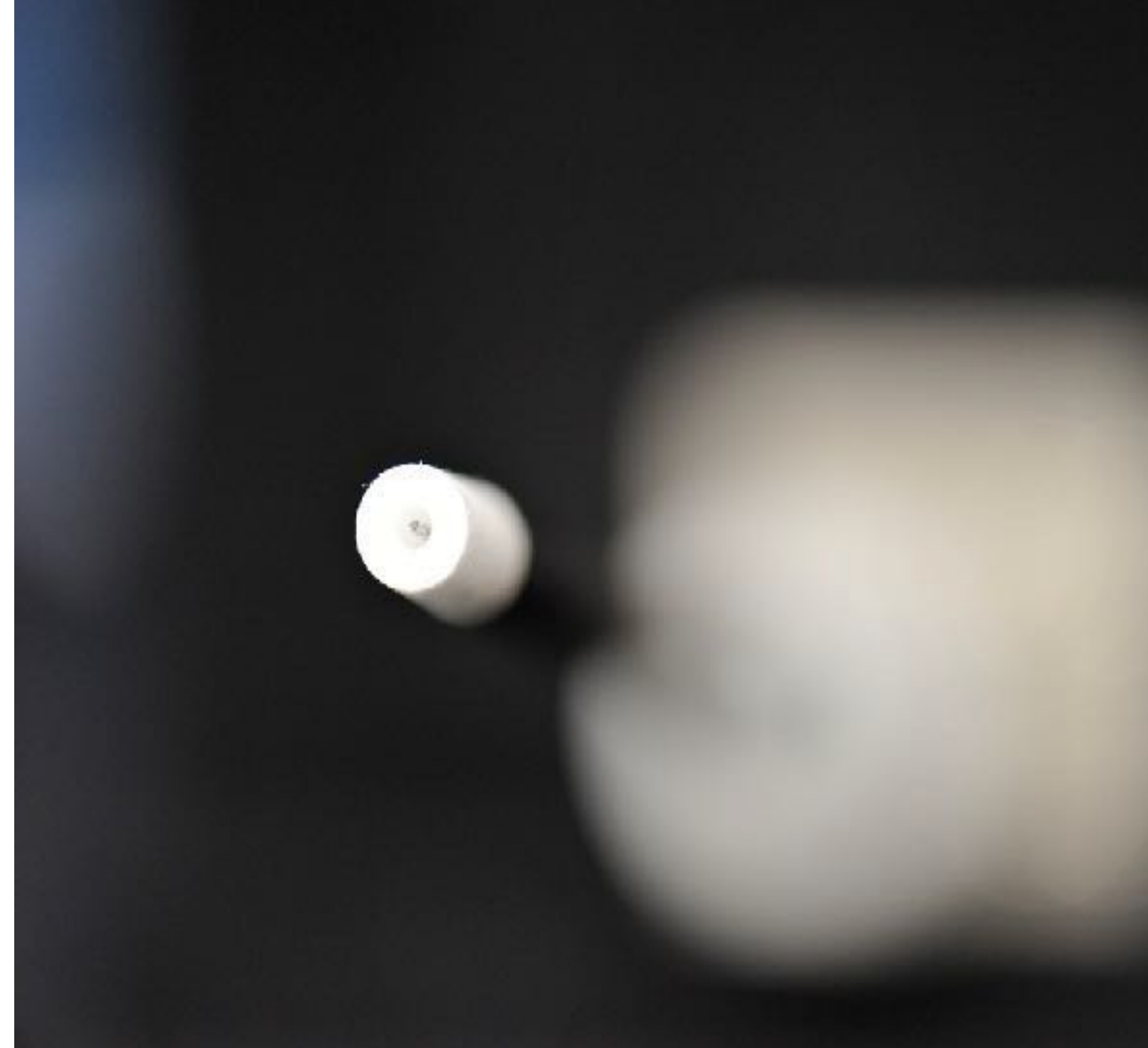


EUmmWV2 Probe: Numerical Optimization



EUmmWV2 Probe Performance

- frequency range: 750 MHz – 110 GHz
- dynamic range: <20 – 10,000 V/m with PRE-10 (minimum <50 – 3000 V/m)
- deviation from hemispherical isotropy: <0.5 dB at 60 GHz
- linearity: <0.2 dB
- compatibility: 5G-Module 1.0+ (DASY6) V1, mmW-Module 1.0+ (ICE V2.0+)
- ISO17025 Calibrated



EUmmW Probe: System Integration in DASY6 & ICEy



Probe Calibration 10 – 110 GHz

Step 1: determining parameters of the sensor model $f(\text{frequency})$

Step 2: determine deviation and isotropy

Traceable Calibration Field >6GHz

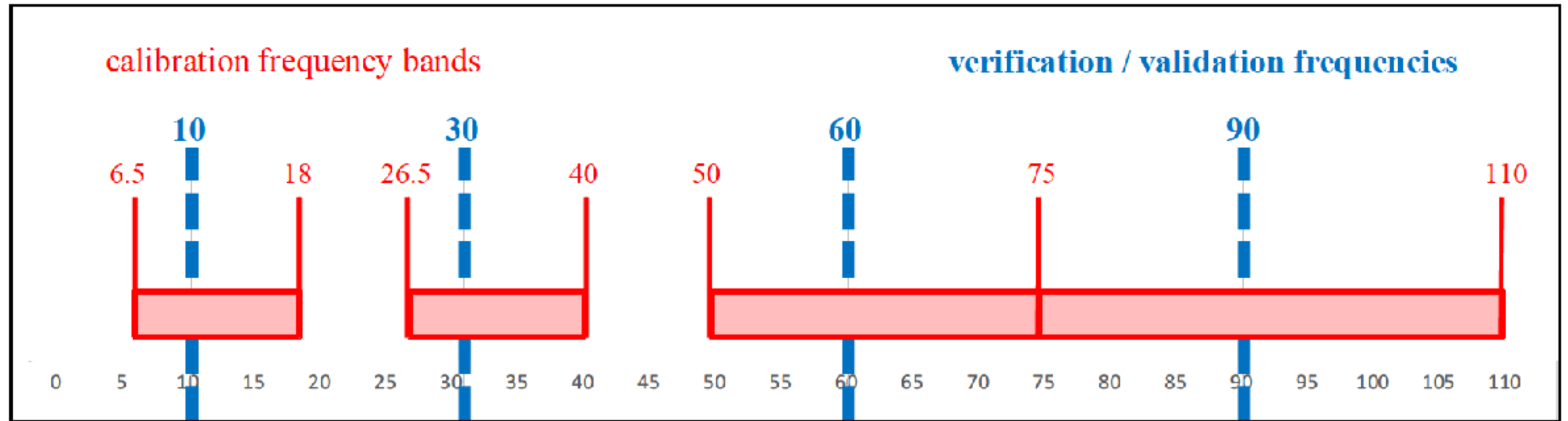
- 3-antenna method
 - 2 horn antennas for transmitter and receiver
 - probe as third antenna
 - advantages over TEM cell or waveguide methods

applied procedure

- step 1:
 - determine phase center vs. frequency by measuring at different distances
- step 2:
 - remove receiver horn
 - insert probe at calibration point
 - probe is outside reactive near field





Calibration System: Sensor Model Calibration (0.75 - 110 Ghz)



Calibration System: ISO17025 Accreditation

- calibration uncertainty: $< \pm 1.0$ dB
- frequency range: 750 MHz – 100 GHz
- ISO/IEC 17025 accreditation
 - received in May 2018

Calibration Laboratory of
Schmid & Partner
Engineering AG
Zughaardstrasse 42, 8694 Zurich, Switzerland

  **S** Schweizerischer Kalibrierdienst
C Service suisse d'etablissement
S Servizio svizzero di taratura
Swiss Calibration Service

Accredited by the Swiss Accreditation Service (SAS)
The Swiss Accreditation Service is one of the signatories to the SA
Multilateral Agreement for the recognition of calibration certificates

Accreditation No.: **SCS 0100**

Client: **ITIS Foundation** Certificate No.: **EUMmWV1-9210_May16**

CALIBRATION CERTIFICATE

Object: **EUMmWV1 - SN 9210**

Calibration procedure(s): **QA CAL-02 v6, QA CAL-25 v6, QA CAL-42 v0.2**
Calibration procedure for E-field probes optimized for close near field
evaluations in air

Calibration date: **May 2, 2016**

This calibration certificate documents the traceability to national standards, which realize the physical units of measurement (SI).
The measurements and the uncertainties with confidence probability are given on the following pages and are part of the certificate.

All calibrations have been conducted in the closed laboratory facility: environment temperature $(22 \pm 1)^\circ\text{C}$ and humidity $\leq 70\%$.

Calibration Equipment used (MATE critical for calibration)

Primary Standards	ID	Cal Date (Certificate No.)	Scheduled Calibration
Power meter NRP	SN: 104728	08-Apr-16 (No. 217-02288/02289)	Apr-17
Power sensor NRP-Z91	SN: 105244	08-Apr-16 (No. 217-02288)	Apr-17
Power sensor NRP-Z91	SN: 105245	08-Apr-16 (No. 217-02289)	Apr-17
Reference 20 dB Attenuator	SN: 85277 (20)	08-Apr-16 (No. 217-02288)	Apr-17
Reference Probe ER15DA6	SN: 2338	13-Jun-15 (No. RRS-1506_Cal15)	Oct-16
UN&T	SN: 908	8-Apr-16 (No. UN&T-908_Apr16)	Apr-17
Secondary Standards	ID	Check Date (in house)	Scheduled Check
Power meter E4410B	SN: 0841203876	08-Apr-16 (No. 217-02288/02289)	In house check: Jun-16
Power sensor E4412A	SN: MY41460087	08-Apr-16 (No. 217-02288)	In house check: Jun-16
Power sensor E4412A	SN: 002118210	08-Apr-16 (No. 217-02288)	In house check: Jun-16
RF generator HP 6642D	SN: U00842001700	04-Aug-09 (in house check Apr-13)	In house check: Jun-16
Network Analyzer HP 8753E	SN: U0537300885	18-Oct-01 (in house check Oct-15)	In house check: Oct-16

	Name	Function	Signature
Calibrated by:	Pat Schott	Deputy Technical Manager	
Approved by:	Raja Hekovic	Technical Manager	

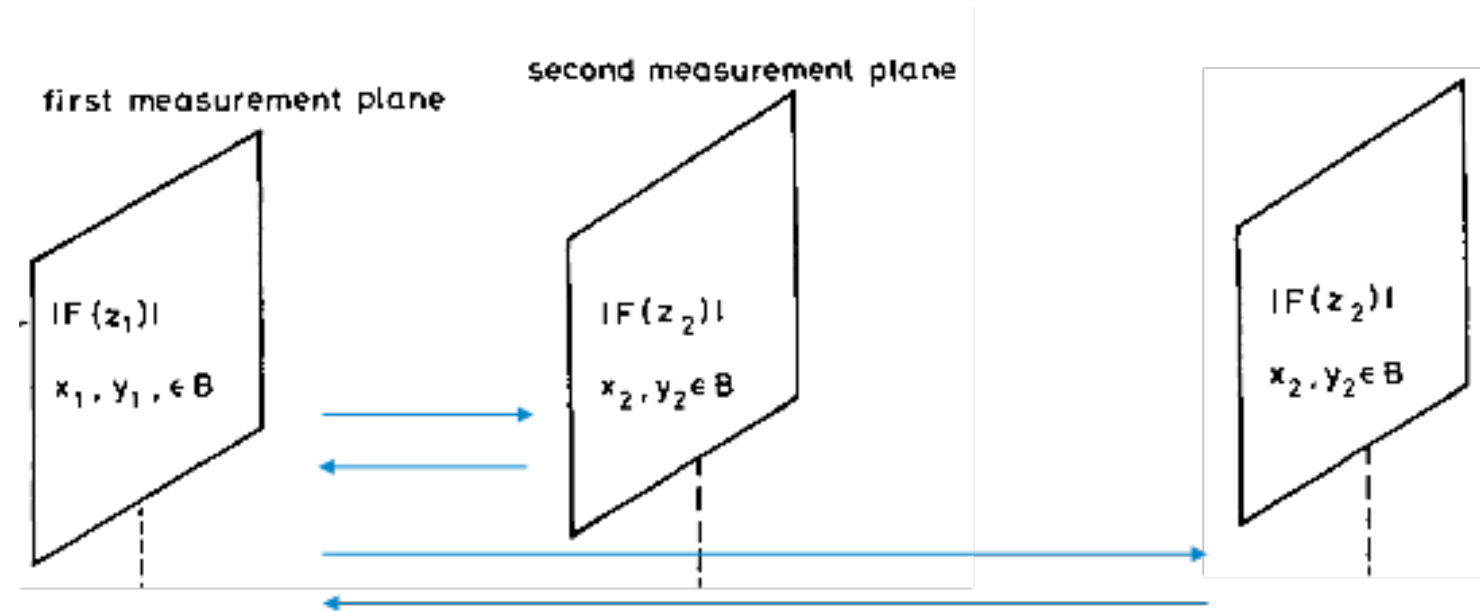
Issued: May 19, 2016

This calibration certificate shall not be reproduced except in full without written approval of the laboratory.

Certificate No: EUMmWV1-9210_May16 Page 1 of 5




Scanning and Field Reconstruction

Reconstruction



- knowledge of E-field distribution on 2 planes allows reconstruction of phase
- plane wave decomposition in infinite plane by Fourier transformation and subsequent reconstruction of full-wave 3D distributions
- our solution for phase reconstruction
 - novel and Improved algorithm based on Gerchberg–Saxton (GS) (R. W. Gerchberg and W. O. Saxton, “A practical algorithm for the determination of the phase from image and diffraction plane pictures,” Optik 35, 237 (1972))
- measurement requirement:
 - 2 planes (grid-step $\lambda/4$): $2 \times 24 \times 24$ points

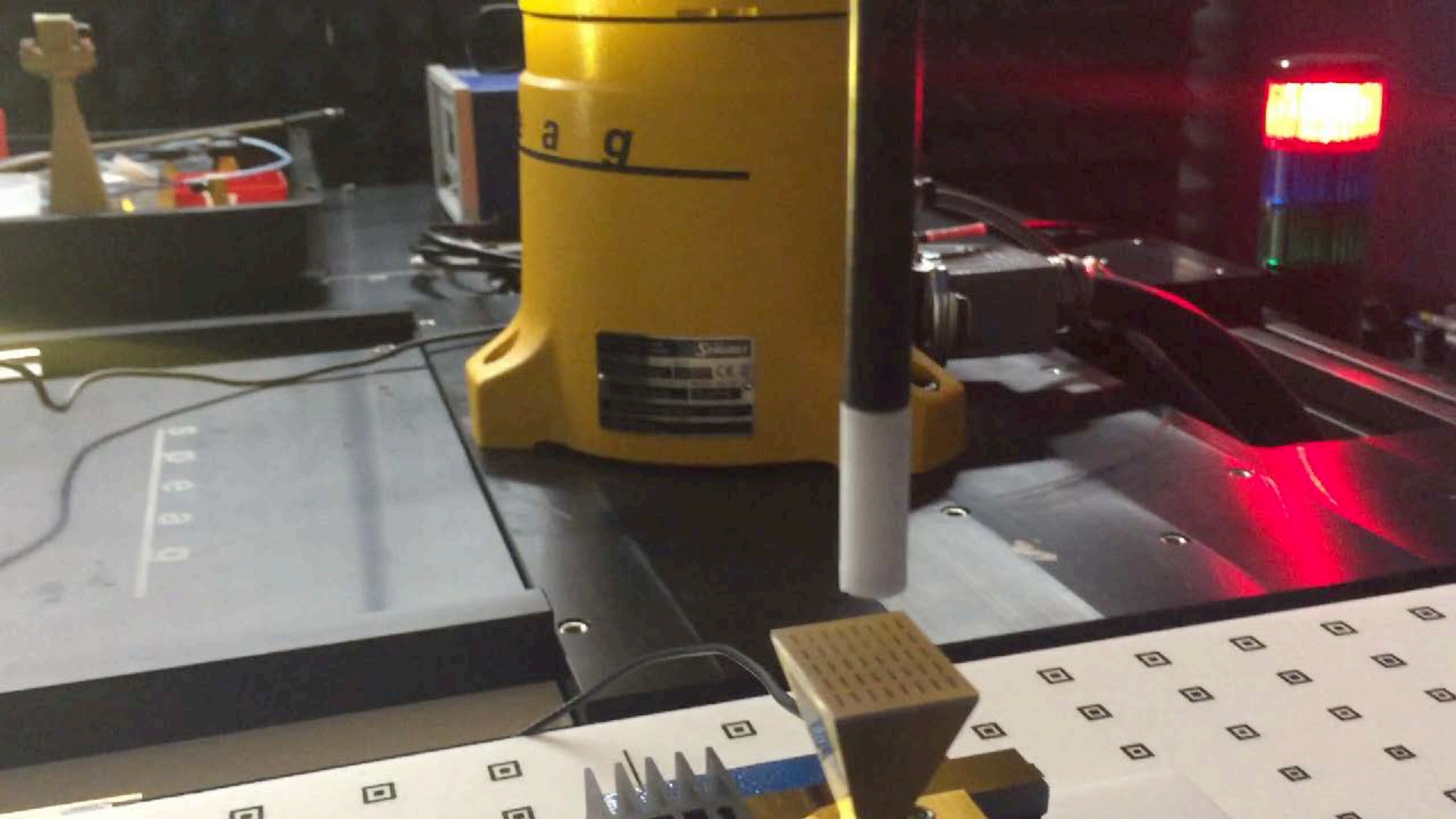
Total Field Reconstruction in the Near Field Using Pseudo-Vector E -Field Measurements

Serge Pfeifer , Eduardo Carrasco , *Senior Member, IEEE*, Pedro Crespo-Valero, Esra Neufeld, Sven Kühn, Theodoros Samaras, Andreas Christ, Myles H. Capstick , and Niels Kuster, *Fellow, IEEE*

Abstract—Exposure assessments in the frequency range above 10 GHz typically require knowledge of the power density very close to the radiator (at 2-mm distance), which can be obtained through the total electric and magnetic fields. However, phase measurements are often not feasible in this frequency range, in particular in the reactive near field. We developed a novel phase reconstruction approach based on plane-to-plane reconstruction algorithms. It uses E -field polarization ellipse information, which can be obtained extremely close to the source with probes based on the pseudo-vector sensor design. The algorithm's robustness and accuracy were analyzed and optimized for distances of a fraction of the wavelength λ , and a comprehensive set of realistic exposure conditions was simulated to evaluate the algorithm. For distances greater than $\lambda/5$, the error of the spatially averaged peak incident

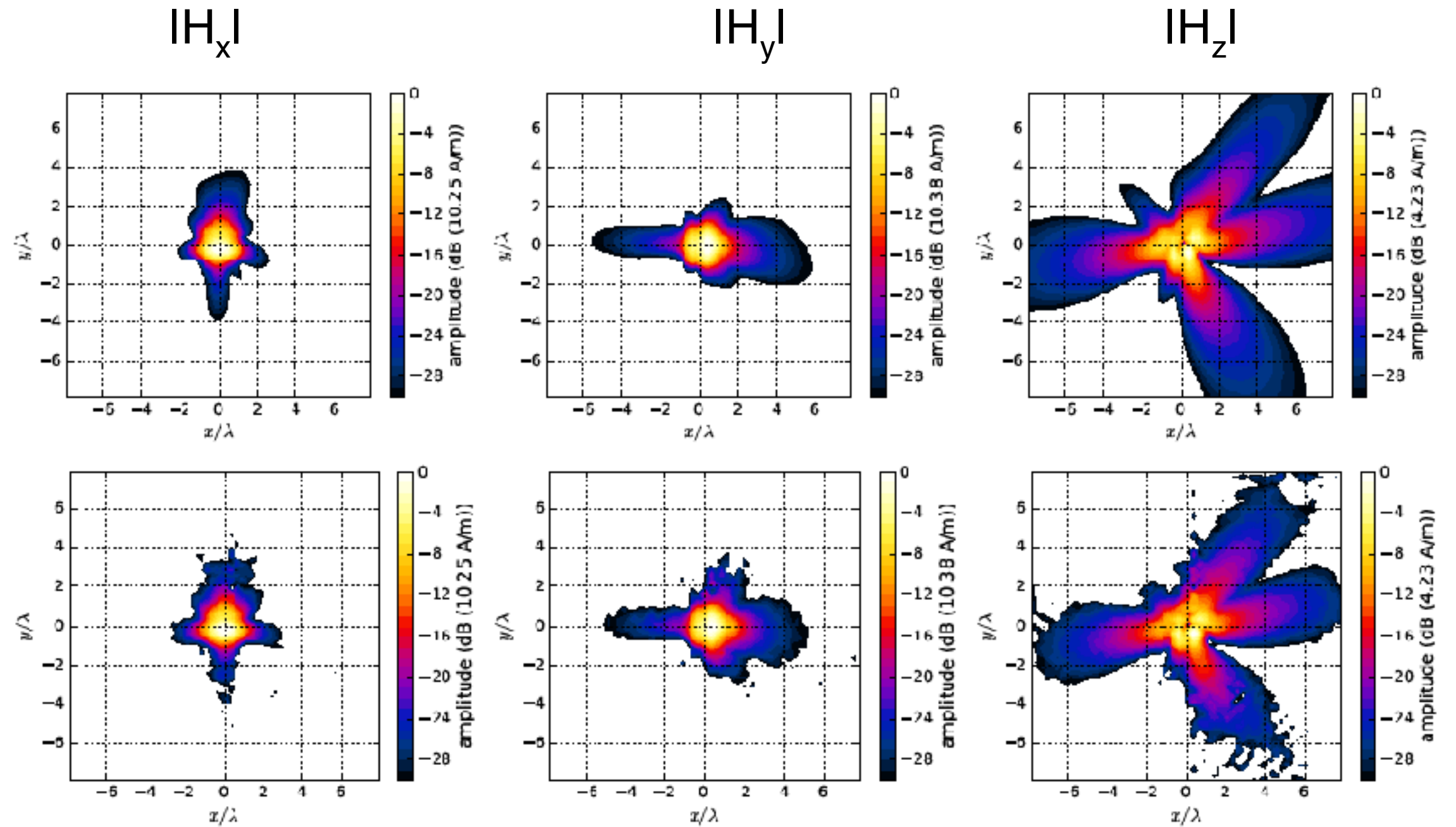
Human exposure to millimeter-wave sources has so far mainly been considered as a far-field problem, but it becomes a near-field problem with integration into mobile devices. This presents potential problems regarding the introduction of 5G technology, as current safety guidelines [1] may not be appropriate for localized sources. Furthermore, there is a lack of measurement equipment available to test compliance very close to 5G millimeter wave devices with regard to current safety guidelines, i.e., the averaged power density S incident to human skin.

Computation of S , in general, requires knowledge of the complex E - and H -field vectors in the plane of incidence. Further-



Example: Magnetic (H-) Field Reconstruction (Distance $\lambda/2$)

reference
(simulation)



reconstruction

Worst-Case Phase Assessment

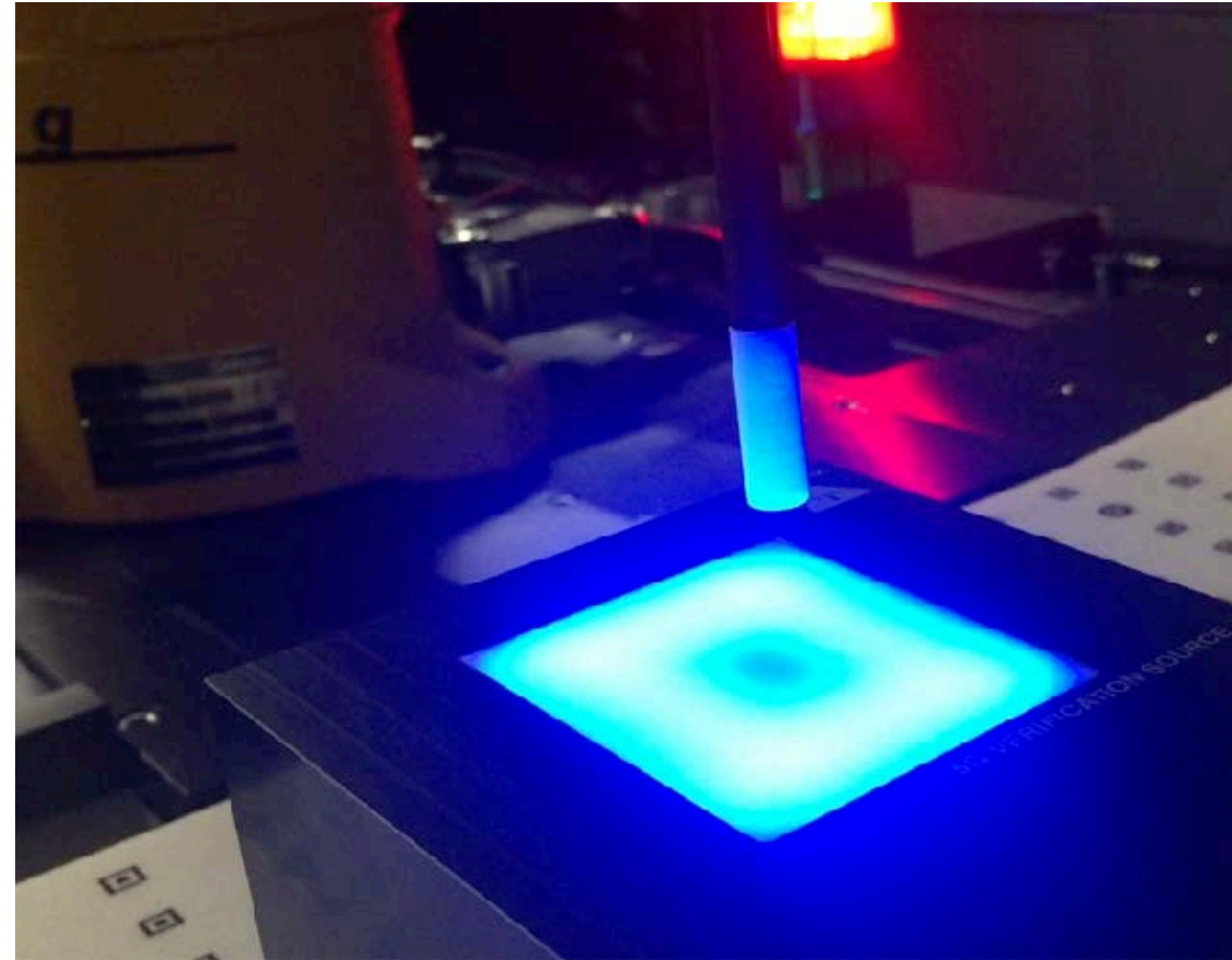
Procedure to Determine Worst-Case Exposure Based on Measurements Only

- measurement of each antenna structure that has a fixed phase correlation (one or more antenna element)
- optimizer for max PD for any phase or subphase range
 - general purpose optimizer
 - Semi-Definite Programming (can only maximize normal component of power density)
- compute forward propagation for all phase configurations using closest measurement plane
- benefit 1: no computation needed -> smaller uncertainty
- benefit 2: computation on any surface by forward propagation
- benefit 3: have full radiation pattern for any phase, beam envelope

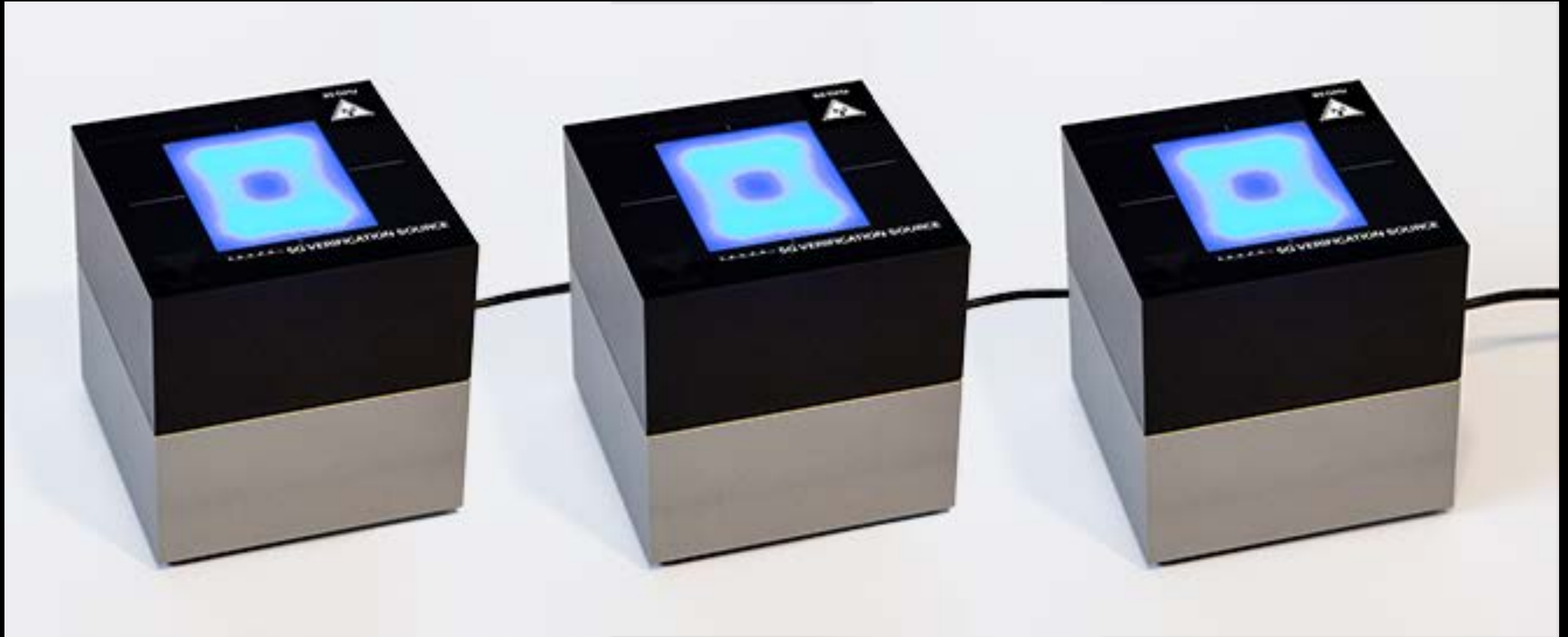
Verification Sources

5G System Verification Packages: 10, 30, 60, and 90 GHz

- 10 GHz: 8.2 – 12.4 GHz horn, SMA female interface, enclosed
- 30, 60, and 90 GHz: stand-alone fixed-frequency sources integrated with horns, enclosed, 12 V DC supply
- compliant with IEC106 AHG10
- release: October 17, 2017



Verification Sources 30, 60 and 90 GHz



Uncertainty Budget

Preliminary Uncertainty Budget

Preliminary 5G Module V1.0Beta Uncertainty Budget Evaluation Distances to the Antennas ≤ 50 mm and the Frequency Range 28 – 90 GHz Based on the 62209 Standard Family						
Error Description	Uncertainty Value (\pm dB)	Probability Distribution	Div.	(c_i)	Std. Unc. (\pm dB)	(v_i) v_{eff}
Measurement System						
Probe Calibration ^c	0.43	N	1	1	0.43	∞
Hemispherical Isotropy	0.60	R	$\sqrt{3}$	1	0.35	∞
Linearity	0.2	R	$\sqrt{3}$	1	0.12	∞
System Detection Limits	0.04	R	$\sqrt{3}$	1	0.02	∞
Modulation Response ^{'''}	0.1	R	$\sqrt{3}$	1	0.06	∞
Readout Electronics	0.01	N	1	1	0.01	∞
Response Time	0.03	R	$\sqrt{3}$	1	0.02	∞
Integration Time	0.11	R	$\sqrt{3}$	1	0.06	∞
RF Ambient Noise	0.04	R	$\sqrt{3}$	1	0.02	∞
RF Ambient Reflections	0.21	R	$\sqrt{3}$	1	0.12	∞
Probe Positioner	0.04	R	$\sqrt{3}$	1	0.02	∞
Probe Positioning	0.11	R	$\sqrt{3}$	1	0.06	∞
S_{avg} Reconstruction ^f	0.61	R	$\sqrt{3}$	1	0.35	∞
Test Sample Related						
Power Drift	0.21	R	$\sqrt{3}$	1	0.12	∞
Power Scaling ^g	0.0	R	$\sqrt{3}$	1	0.0	∞
Combined Std. Uncertainty					0.7	∞
Expanded Std. Uncertainty					1.4	

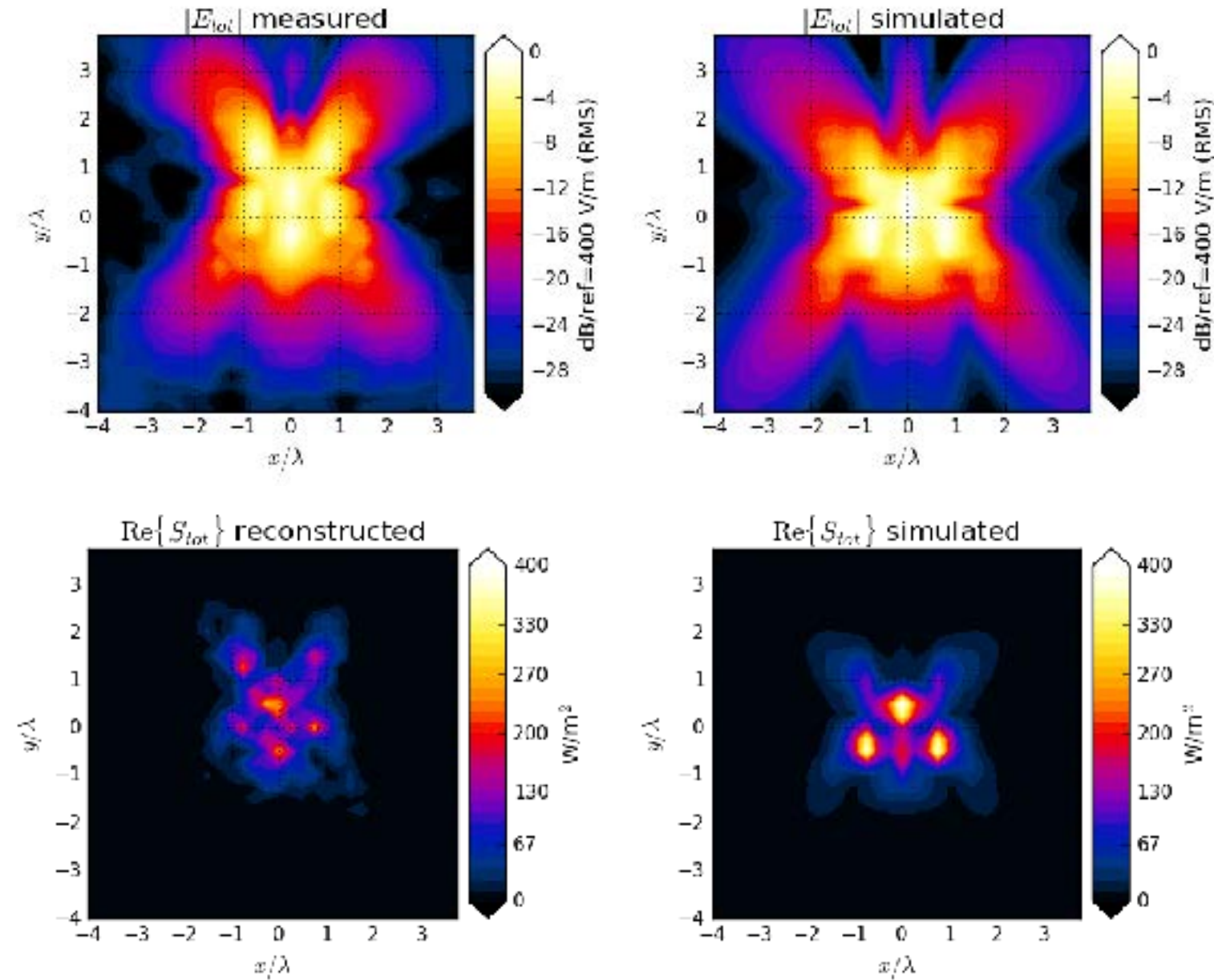
System Validation

Cavity Backed Array of Dipoles – 30 GHz



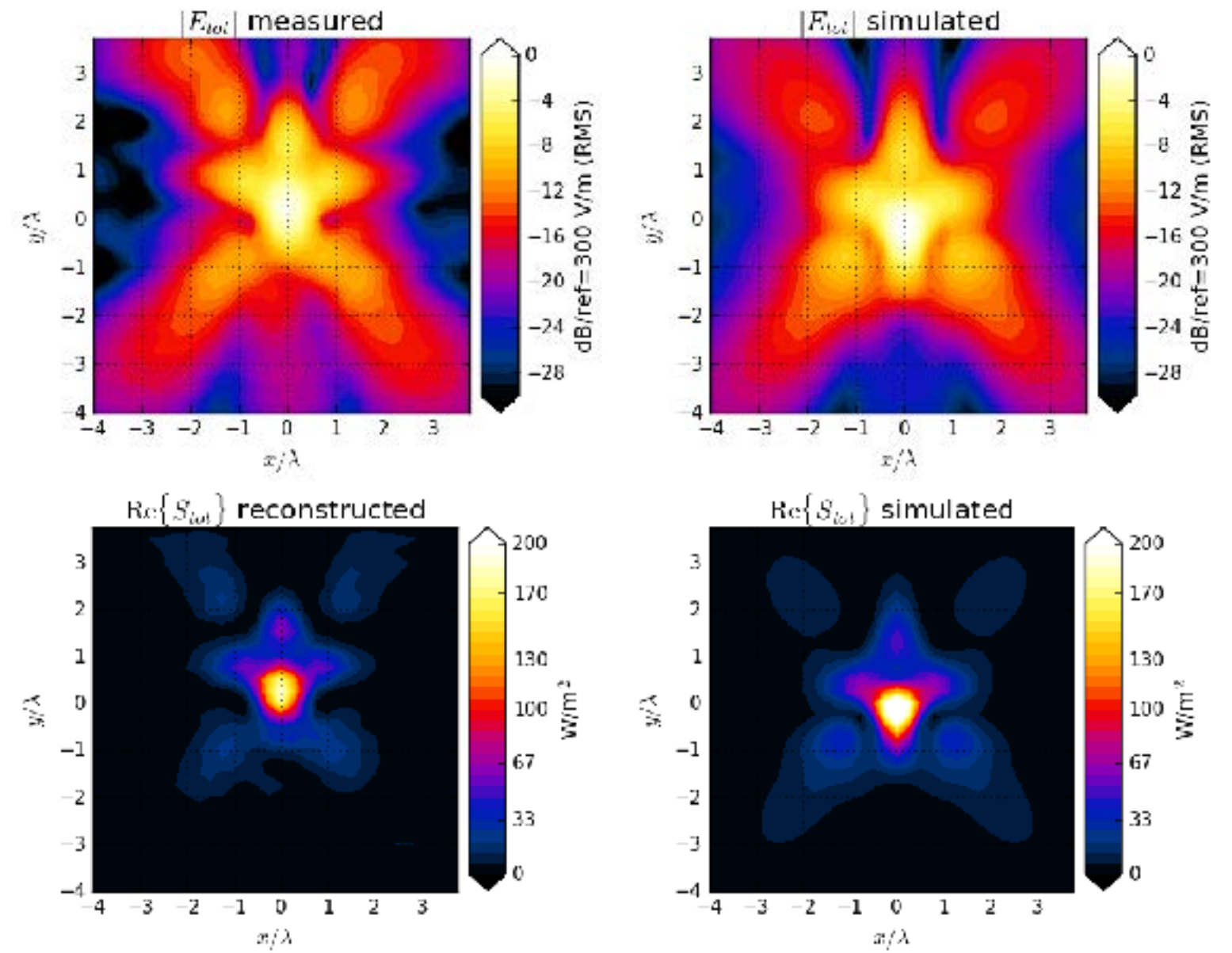
2 mm

2 mm



10 mm

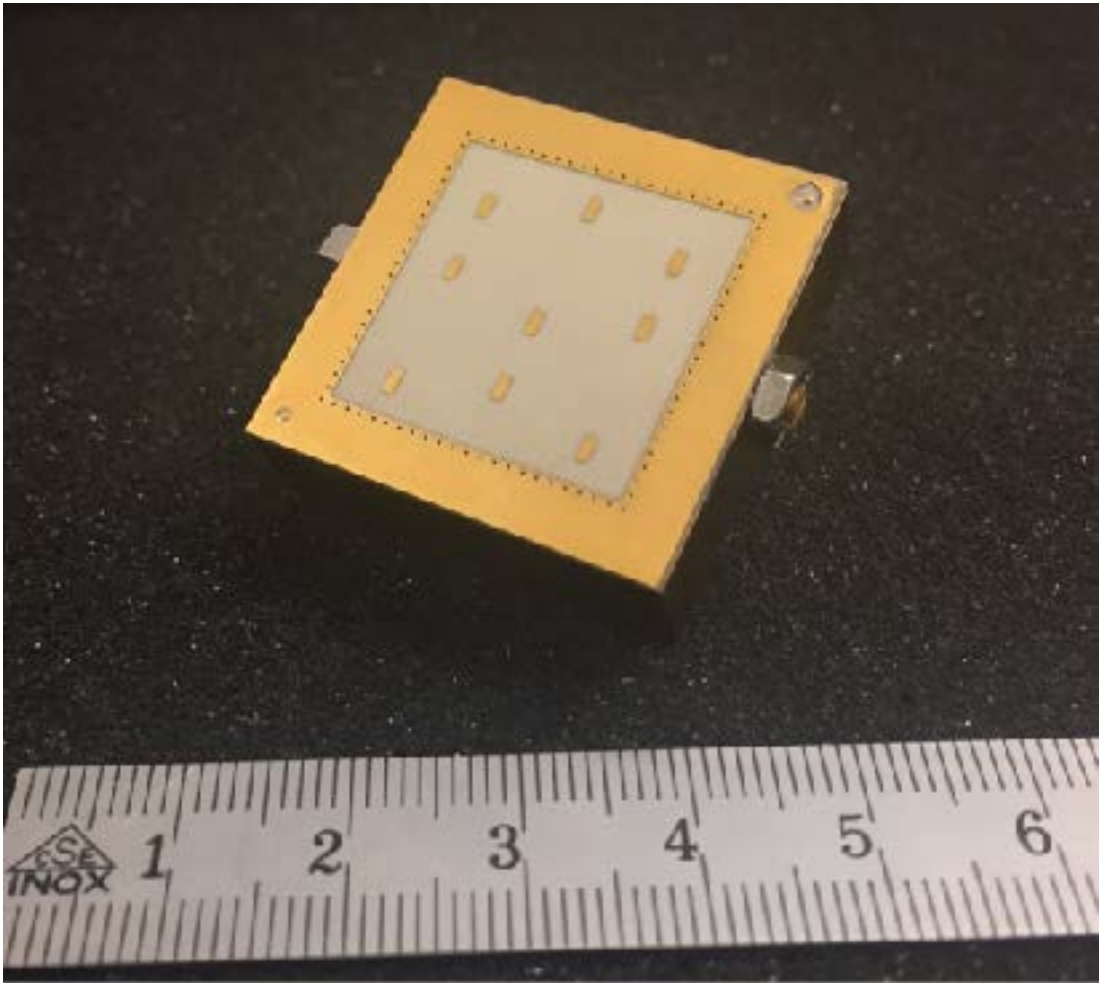
10 mm



Validation Results: Cavity Backed Array of Dipoles – 30 GHz

■ normalized to 10 dBm

distance (mm)	simulated		measured		deviation	
	E_{total} (V/m)	S_{avg} 1 cm ² (W/m ²)	E_{total} (V/m)	S_{avg} 1 cm ² (W/m ²)	E_{total} (dB)	S_{avg} 1 cm ² (dB)
2	422.54	131.37	374.38	112.43	-1.1	-0.7
4.5	269.02	116.31	290.79	89.77	0.7	-1.1
10	303.64	119.83	278.91	101.38	-0.7	0.7
12.5	302.29	121.05	263.08	94.2	-1.2	-1.1
50	121.32	36.31	121.32	33.6	0.0	-0.3



Preliminary Results: Pyramidal Horn with Slot Array – 60 GHz

distance /(mm)	simulated		measured		deviation	
	E_{total} (V/m)	S_{avg} 1 cm ² (W/m ²)	E_{total} (V/m)	S_{avg} 1 cm ² (W/m ²)	E_{total} (dB)	S_{avg} 1 cm ² (dB)
2	196.7	54.46	210.44	49.43	0.59	-0.4
3.25	177.11	50.34	203.61	43.41	1.21	-0.6
10	154.85	39.28	159.97	36.27	0.28	-0.4
11.25	145.43	37.55	152.3	34.62	0.4	-0.4
50	88.74	18.23	88.73	17.12	0	-0.3



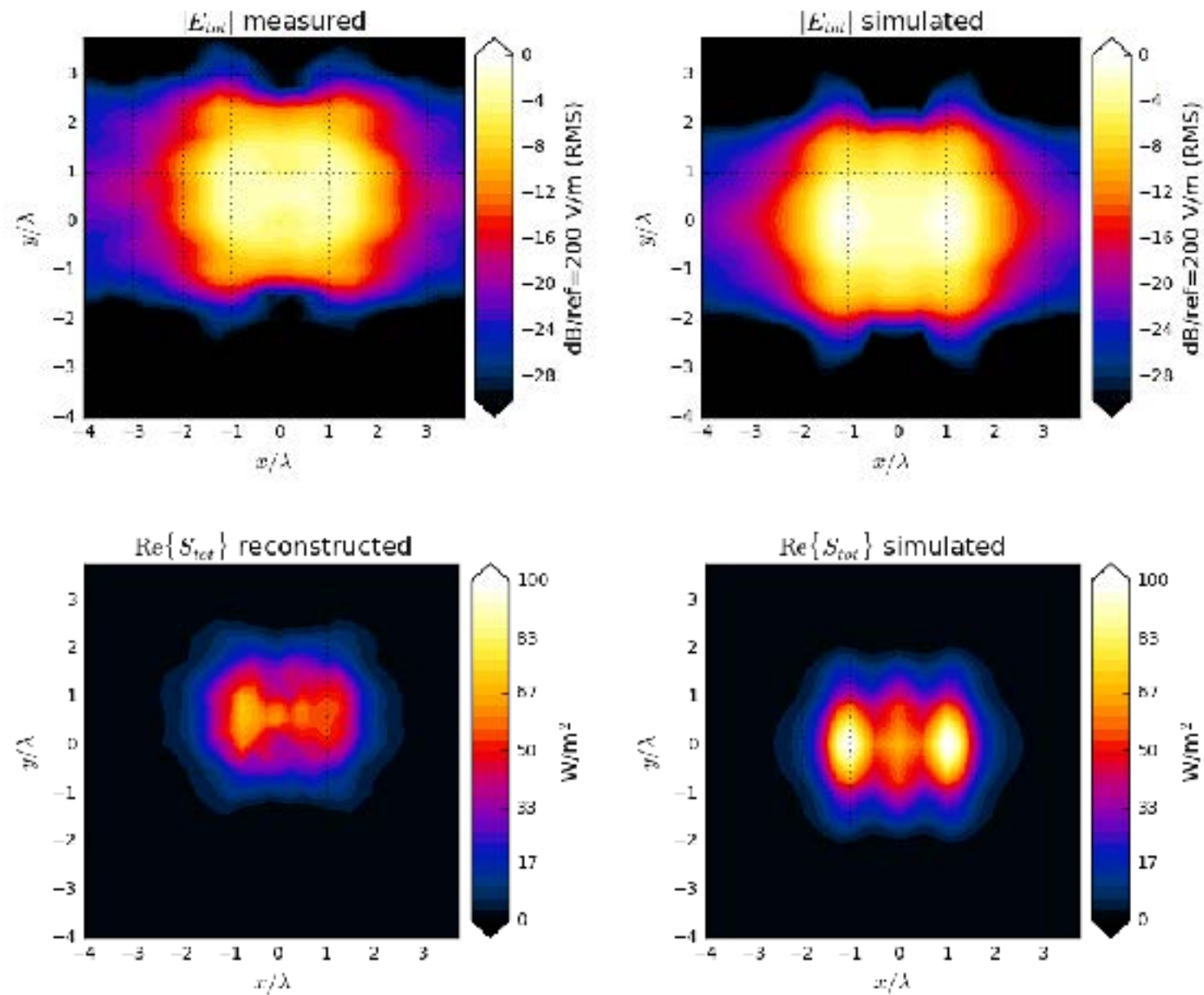
Preliminary Results: Pyramidal Horn with Slot Array – 90 GHz

distance /(mm)	simulated		measured		deviation	
	E_{total} (V/m)	S_{avg} 1 cm ² (W/m ²)	E_{total} (V/m)	S_{avg} 1 cm ² (W/m ²)	E_{total} (dB)	S_{avg} 1 cm ² (dB)
2	192.72	45.5	161.79	35.79	-1.5	-1.0
2.83	179.57	43.78	171.37	39.21	-0.4	-0.5
5	167.92	39.28	164.56	34.81	-0.2	-0.5
5.83	161.32	37.85	166.12	33.36	0.3	-0.6
10	118.79	29.58	123.3	27.19	0.3	-0.4
10.83	118.78	28.29	112.71	25.23	-0.5	-0.5

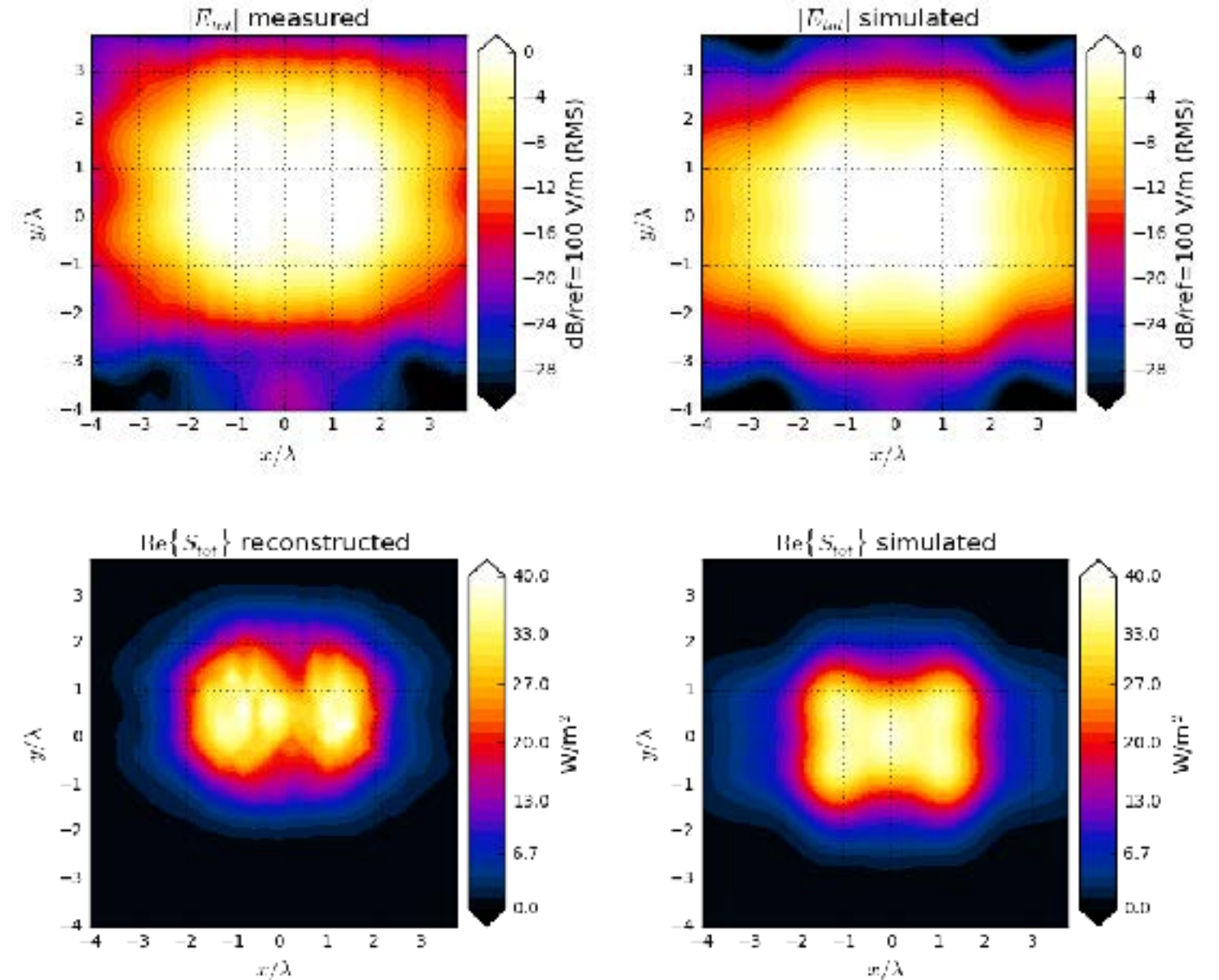
Pyramidal Horn Loaded with Slot Array, 90 GHz



2 mm



10 mm



Combination of SAR & Power Density

SAR & PD Combiner Feature (Simultaneous Transmissions)

- fast volume SAR for each transmission mode
- PD evaluation on the surface of the phantom
- combining all simultaneous transmission point exposures in the 3D volume

$$\frac{\text{Power Density}}{\text{Power Density Limit}} + \frac{SAR_{1g/10g}}{SAR_{1g/10g} \text{ Limit}} < 1$$

- fast and accurate method without overestimations

Conclusions

Conclusion: 5G Solutions (>6 GHz)

- novel EUmmW probe
- novel reconstruction algorithm validated $>\lambda/5$
- traceable calibration
- system check sources
- validation sources
- system validated for $\geq 2\text{mm}$ from 30 GHz
- uncertainty: ~ 0.7 dB ($k=1$)
- further improvements in research and development

Conclusion Standard

- latest research indicates that the currently proposed limits may not prevent thermal tissue damage (additional review needed)
- epithelial power density at body surface (W/m²) for >6GHz can be considered to equivalent to SAR (however, keeping SAR would be the better choice)
- SAR and epithelial power density can be measured up to 10 GHz in phantoms (extension to 20 GHz is feasible)
- free space PD can be only accurately assessed and is correlated to induced field as close as 2mm & $\lambda/5$
- integral of the norm is not always conservative
- worst-case assessment can be achieved by measurement only
- proposed limits are not always consistent with latest research and need to be reviewed

■ **note: we are hiring ambitious PhD Students and Postdocs**